

Gross and Microscopic Lesions in the Female SENCAR Mouse Skin and Lung in Tumor Initiation and Promotion Studies

by Gary L. Knutsen,* Robert M. Kovatch,* and Merrel Robinson[†]

The skin and lung tissues from SENCAR mice used as part of the Environmental Protection Agency's (EPA's) Carcinogenesis Testing Matrix were examined. This study included SENCAR mice used in three different short-term bioassay protocols in which the skin papilloma assay was used to identify initiators, promoters, and complete carcinogens. Also included were the pathology findings from SENCAR mice used in the combined bioassay in which the skin assay and the lung adenoma assay were conducted simultaneously. The gross and microscopic features of treatment-associated and spontaneous lesions of the skin and lung of the SENCAR mouse used in these studies are defined and the lesions most commonly observed are described.

Generally, gross observations and microscopic findings in both the skin and lung tissues were poorly correlated. Although there are several definite criteria on which gross interpretations of the various skin and lung lesions can be made, with the exception of pedunculated squamous cell papillomas and the classic squamous cell carcinomas, the various lesion types had a wide variety of clinical presentations that severely compromised the accuracy of gross diagnosis. Further, in the case of benign skin neoplasms, malignant transformation of these tumors most often occurred at the base of the lesion and was initially hidden from gross observation. As a result, approximately 50% of the neoplasms interpreted clinically as benign tumors (papillomas and keratoacanthomas) were actually malignant neoplasms. Moreover, many lesions determined grossly to be nontumorous were in fact found to be neoplastic when examined microscopically.

The SENCAR mouse was found to be more responsive in the lung adenoma assay than other strains examined with exception of the Strain A. Although accurate interpretation of the lung lesions in the SENCAR was compromised by nonneoplastic treatment-associated and/or spontaneous lesions, the feasibility of using the SENCAR skin and lung as target tissues in two-stage combined carcinogenesis studies merits further consideration.

Introduction

The concept of two-stage chemical carcinogenesis was first identified by Berenblum (1) and Rous (2) in 1941. Much of our understanding of the mechanisms of this concept has been gained from the mouse skin papilloma assay (3-6). Although a variety of strains of mice have been used in the assay, the SENCAR mouse, a stock bred specifically for its sensitivity to two-stage skin carcinogenesis, has been most frequently used in these studies. Slaga has shown the SENCAR mouse to be the most sensitive mouse skin carcinogenesis system for the identification of initiators, promoters, and more recently, complete carcinogens (7). This sensitivity has been confirmed by other investigators (8-10). Based on these findings, the Environmental Protection Agency,

Health Effects Research Laboratory (EPA/HERL), included the SENCAR Skin Papilloma Assay in the bank of short-term bioassays that make up the EPA's Carcinogenesis Testing Matrix, a program of Tier 2 bioassays designed to confirm the carcinogenic properties of environmental chemicals and mixtures (11). Robinson and others, in an attempt to consolidate several of the assays and improve sensitivity (12), recently reported the use of the SENCAR mouse in a combined bioassay in which the skin papilloma assay was conducted simultaneously with a modified version of the lung adenoma assay, a test traditionally conducted in Strain A mice (13,14).

Although the responsiveness of the SENCAR Skin Papilloma Assay has been reviewed and is well documented for a wide variety of chemicals (4,8-11,15), and the sensitivity of the lung has been reported in the SENCAR mouse for several chemicals (12), little information has been published on the pathology of the lesions induced in both the skin and lung of SENCAR mice in these assays. Moreover, most of the published

*Pathology Associates, Inc., 10075 Tyler Place, Hyatt Park II, Ijamsville, MD 21754.

[†]Toxicology and Microbiology Division, Health Effects Research Laboratory, Environmental Protection Agency, Cincinnati, OH 45268.

pathology reports of skin carcinogenesis in the SENCAR mouse have involved the microscopic confirmation of a percentage of skin lesions as carcinomas or were limited to those identified clinically as carcinomas. There is a paucity of information concerning the diagnostic criteria on which gross observations were based, and microscopically, classification of the skin neoplasms in these reports was limited to "papilloma" and "carcinoma." To date, no reports concerning the induced or spontaneously occurring pulmonary lesions of SENCAR mice have been published.

During the past 30 months, we have evaluated, by both gross and microscopic examination, the skin and lung tissues from more than 12,000 female SENCAR mice as part of the EPA's Tier 2 Matrix studies for two-stage carcinogenesis. It is the purpose of this paper to provide diagnostic criteria and morphologic descriptions of the gross and microscopic treatment-induced lesions in the SENCAR mouse skin and lung.

Materials and Methods

Experimental Design

The pathological findings described represent treatment-induced lesions observed in female SENCAR mice used in EPA's two-stage Carcinogenesis Testing Matrix project. The four basic types of protocols used in the SENCAR Matrix studies have been previously described in detail (12,15-17) and included the following: Protocol 1: initiation/promotion (tumor initiators) skin papilloma assay; Protocol 2: initiation/promotion (promoting agents) skin papilloma assay; Protocol 3: complete carcinogenicity skin papilloma assay; Protocol 4: combined bioassay; skin papilloma and lung adenoma assays.

The first protocol, designed to test the initiating potential of a substance, consisted of the exposure of female SENCAR mice to either single or multiple doses of chemical or environmental mixture applied topically or subcutaneously to the shaved dorsal skin of the mouse. Two weeks following initiation, the promoting agent, 12-O-tetradecanoylphorbol-13-acetate (TPA) was administered (1 μ g/application in 0.2 mL acetone) three times a week for 20 weeks. Protocol 2 was the same, with the exception that a known initiator, urethane, was followed by 20 weeks of application with the suspected promotor. For Protocol 3, the test substance was administered three times per week to the dorsal skin of animals, either topically or subcutaneously, for a period of 1 to 20 weeks to test for complete carcinogenic properties. For the combined bioassay (Protocol 4), two days after a single dose of a known carcinogen was administered by intraperitoneal injection, 1.0 μ g of TPA was applied three times a week for 20 weeks.

The appearance and regression of skin tumors were charted weekly using a grid system with letter and number coordinates to permit specific lesions to be identified by size and topography. For Protocols 1, 2, and 3, the animals were typically sacrificed 12 months following

initiation or at approximately 14 months of age. The animals were 36 weeks of age at sacrifice for the Combined Bioassay studies.

Clinical Observations

Following quarantine of the mice, the test animals were identified, weighed, shaved, and placed into treatment groups. The mice were shaved weekly thereafter to facilitate administering test compounds and lesion observation. After the initial weighing, the animals were weighed each week for 6 weeks, then monthly for the duration of the study.

During the course of the study, two daily observations of the animals were made to check food and water and to monitor morbidity. In addition, a weekly observation was performed on all test animals during which all grossly observed lesions were charted on a grid, and the lesion type, location, and size were indexed. Based on clinical observations and standardized morphologic criteria, the lesions were placed by type into one of four categories: papilloma, carcinoma, sore, and subcutaneous lesion. All nontumor lesions, including ulcers, erosions, etc., were categorized as sores. Lesions were classified as subcutaneous if the skin over the lesion was intact. During the weekly observations, all lesions identified as tumors were recorded and included in the daily count. When tumors were observed for three consecutive weeks, the tumor counts were included in the cumulative counts. All individual tumors were charted weekly until they regressed or coalesced, or until the animal either died or was sacrificed.

Test Animals

Female SENCAR mice, from 5 to 8 weeks of age, were obtained from Harlan Sprague-Dawley Inc. (Indianapolis, IN). The animals were quarantined at the EPA facility for a maximum of 2 weeks. Mice were placed on study when the majority of mice were in the resting stage of the hair growth cycle. Depending on protocol, the animals were divided into groups of 20 to 40 animals and housed 10/cage. Water and Purina Lab chow were provided *ad libitum*.

Necropsy

A complete necropsy was performed for all spontaneous deaths, moribund sacrifices, and the scheduled terminal sacrifice. Gross observations of all external and internal lesions were recorded on specially designed necropsy forms that enabled the individual skin lesions to be specifically documented by number, size, and location on the carcass. At least one photograph was taken of each animal to demonstrate each skin lesion and other representative internal gross lesions. Necropsy included examination and fixation of 41 tissues, which, along with the carcass, were placed in 10% neutral buffered formalin. In all studies, the lungs were removed intact, examined for lesions, and perfused to approxi-

mate tidal volume, after which the trachea was ligated. The individual skin lesions were prosected and placed into cassettes to maintain identity. Additionally, a piece of "normal" dorsum skin was also obtained from each mouse. All skin tissues were stretched and mounted on filter paper before fixation.

Histopathology

Microscopic evaluation of tissues for all protocols was limited to the dorsal treatment area, all grossly recognized skin lesions up to six per animal, and all other lesions observed as abnormal either at necropsy or during tissue trimming. In those animals in which multiple skin lesions were present, each lesion was trimmed and processed in a separate cassette to maintain identity of the lesion for subsequent correlation with both clinical observations and necropsy findings. In the combined bioassay, a Shimkin adenoma assay was conducted (13). The lobes of the lung were separated, lesions consistent with primary lung tumors were counted and tabulated, and each lesion was recorded topographically on lung count forms. This task was performed by two technicians working independently of each other. Significant discrepancies were further examined by either the pathologist or a third technician. Unresolved discrepancies, all gross lesions of questionable diagnosis, and at least 10% of the lung tumors were examined microscopically for lesion confirmation and/or diagnosis.

The identity of each skin lesion was maintained throughout the process to enable subsequent correlation of the microscopic findings with the gross observation at necropsy and previous clinical findings. These data were subsequently analyzed to determine the accuracy of skin lesion diagnoses based on gross interpretations. All microscopic diagnoses were entered into a computerized pathology data system that generated the incidence tables for individual animals and summary tables for all animals.

Results and Discussion

Gross and Microscopic Lesions of the Skin and Subcutis

Samples of skin tissues removed from the dorsal treatment area and all skin lesions from more than 12,000 SENCAR mice used in EPA's Matrix studies were examined grossly at necropsy and during tissue trimming and were then evaluated by light microscopy. A wide variety of inflammatory, hyperplastic, and neoplastic lesions were observed in the animals. A list of these lesions, separated into general morphologic classifications, is shown in Table 1. The vast majority of these lesions were very likely treatment-induced with the exception of focal inflammatory and hyperplastic lesions confined to the epidermis and immediately adjacent dermis and several neoplasms of the subcutis that were probably naturally occurring.

Nonneoplastic Lesions of the Skin and Subcutis.

Table 1. Classification of lesions of the skin and subcutis in female SENCAR mice.

Neoplasms	Nonneoplastic lesions
Epidermal neoplasms	Epithelial hyperplasia
Squamous cell papilloma	(acanthosis, hyperkeratosis, parakeratosis)
Pedunculated	Inflammation (acute, subacute, chronic, chronic-active)
Sessile (broad based)	Erosion
Keratoacanthoma	Ulceration
Squamous cell carcinoma	Epidermal inclusion cyst
Keratinizing	Myeloid hyperplasia
Nonkeratinizing	Amyloid
Anaplastic	
Basal cell tumor	
Neoplasms of the subcutis	
Fibroma	
Fibrosarcoma	
Rhabdomyosarcoma	
Plasma cell tumor	
Sarcoma, NOS	
Malignant lymphoma	
Mammary gland neoplasms	
Adenoma	
Adenocarcinoma	
Adenoacanthoma	

The most frequently occurring lesion involving the skin/subcutis in treated animals was inflammation and hyperplasia of the epidermis and dermis. These changes varied from small focal areas of acute inflammation to extensive erosive and/or ulcerative areas accompanied by varying amounts of epithelial hyperplasia, consisting of acanthosis, hyperkeratosis, and parakeratosis (Fig. 1). The epidermal rete pegs, consisting of well organized fingerlike projections of hyperplastic epithelial cells, extended into the dermis and occasionally into the subcutis. Generally, the hyperplastic response was associated with varying amounts of chronic-active inflammation with abundant amounts of keratinaceous debris usually present on the epidermal surface. On gross examination, these lesions were clinically recorded as sores, and were characterized by loss of hair

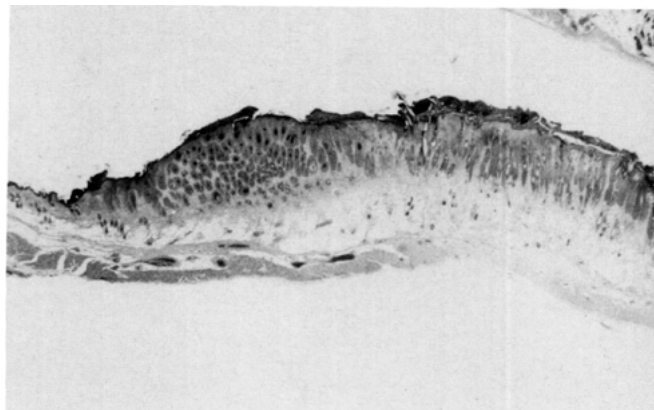


FIGURE 1. Epithelial hyperplasia. Area of severe epithelial hyperplasia consisting of acanthosis and hyperkeratosis with inflammation of the dermis and subcutis. Normal skin is observed at the left margin of the lesion (H & E, $\times 26$).

over what was usually a dry, crusty, slightly raised lesion that may or may not have been ulcerated. The margin of the lesion showed a smooth transition as it blended into the adjacent normal skin.

Focal areas of inflammation and hyperplasia were observed in nontreated mice but never to the extent shown in Figure 1. The small, focal lesions often represented inflammatory response to bite wounds or other local irritation. Other large areas of uniform epithelial hyperplasia not accompanied by either ulceration or inflammation were also observed. These lesions were very likely naturally occurring; however, the development of hyperplasia in response to continued shaving merits consideration. In this paper we provide evidence for the development of neoplasms from hyperplastic lesions, a progression that has been previously documented in mouse skin carcinogenesis studies (18-20). Since we have diagnosed squamous cell papillomas in nontreated mice, it is assumed that at least some of the hyperplastic lesions also occurred spontaneously in the SENCAR mouse.

Another nonneoplastic lesion of the skin, the epidermal inclusion cyst defined by Bogovsky (19), was commonly observed in treated animals and in a few of the nontreated mice. The incidence of these cysts increased with the severity of skin ulceration and the amount of active inflammation. The skin generally remained intact over these lesions, and they appeared clinically as subcutaneous raised areas or nodules. In those cases where the skin surface was interrupted, the lesion was occasionally misinterpreted as a skin neoplasm. In several instances, the usually thin layer of epithelial cells lining the cyst appeared to undergo malignant transformation, and a squamous cell carcinoma was observed within the cyst. If the skin surface remained intact, the latter lesion was not detected clinically.

A high percentage of the treated mice had aggregates of cellular infiltrates in the subcutis consisting of either plasma cells or loosely arranged aggregates of mature and immature cells of the granulocyte series. The latter lesion, diagnosed as myeloid granulocytic hyperplasia, was a proliferative change that is often systemic and is commonly seen in mouse skin paint studies. Historically, this lesion has often been misinterpreted as granulocytic leukemia. The differential features of myeloid hyperplasia versus granulocytic leukemia has been discussed recently by Long (21).

The final nonneoplastic lesion observed in the skin was deposition of amyloid in the dermis immediately adjacent to the basement membrane of the epidermis. This deposition occurred in association with varying amounts of epidermal hyperplasia and was usually accompanied by mild, chronic inflammation of the dermis and subcutis consisting of lymphocytes, macrophages, and varying numbers of plasma cells. The presence of amyloid in the skin is not an unexpected finding, especially since Kovatch (22) has reported amyloid deposition in a wide range of tissues in both treated and nontreated SENCAR mice.

Lesions of the adnexal structures of the skin were

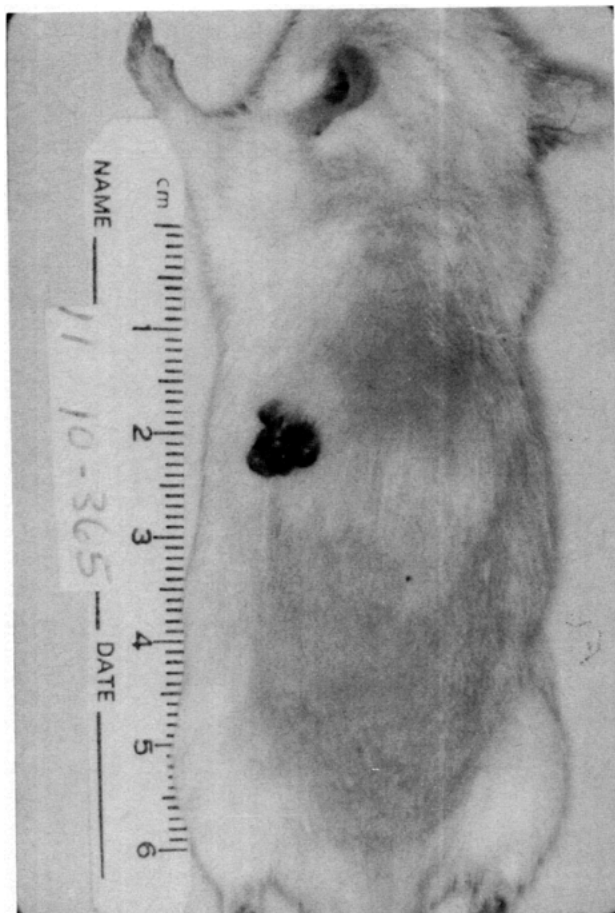


FIGURE 2. Squamous cell papilloma. Single sessile papilloma in a SENCAR mouse with keratinized, cauliflower-like protuberances.

lacking, with the exception of focal inflammation of hair follicles. Although small foci of sebaceous cell differentiation were present in several of the skin tumors, hyperplastic lesions of the sebaceous glands were not observed.

Neoplastic Lesions of the Skin and Subcutis. The most frequently occurring benign neoplasm of the skin observed in the SENCAR Matrix studies was the squamous cell papilloma. This tumor had a variety of clinical presentations and varied in size from 0.1 cm to greater than 2.0 cm in diameter. The papillomas projected above the surface of the skin either as keratinized, pointed protuberances or as lobulated, cauliflower-like growths. The tumors were red to dark tan and had dry, rough, and finely fissured surfaces (Fig. 2). Papillomas were classified into two types by the morphologic features of their attachment to the skin; either pedunculated, having a thin stalk, or sessile, having a broad base with a height less than the diameter of the attachment. Gross examination and palpation of the pedunculated lesion revealed the lesion to be a knoblike growth attached by a stalk of variable thickness with the base of the stalk attachment blending evenly with the skin surface. The broad-based papillomas were more difficult to palpate,

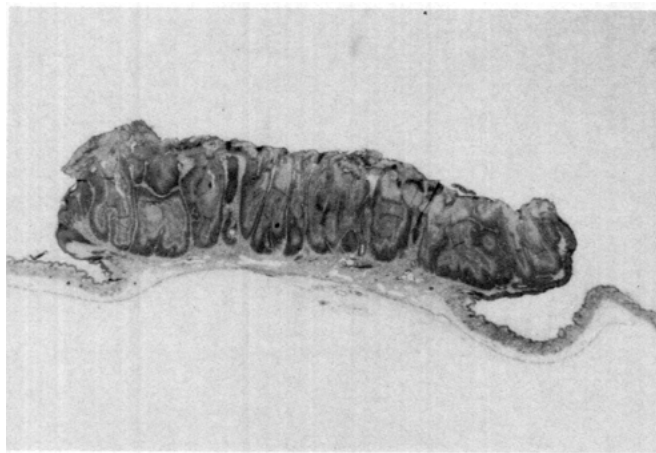


FIGURE 3. Squamous cell papilloma. Typical sessile (broad based) squamous cell papilloma with the diameter of the base of the tumor greater than the height (H & E, $\times 26$).

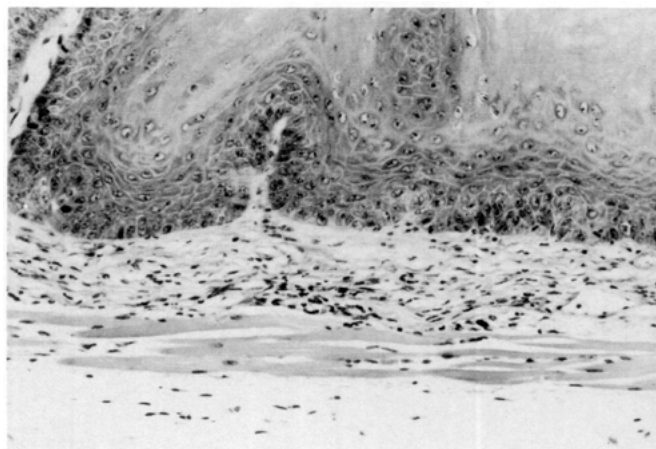


FIGURE 4. Squamous cell papilloma. Base of the sessile papilloma in Fig. 3. The base of the rete ridges are well organized and there is no interruption of the basement membrane (H & E, $\times 260$).

but important diagnostic information was gained by carefully examining the base of the lesion for any irregular growths, acute inflammation, hyperemia, swelling, and/or adherence to the underlying tissue, all of which are indications of malignancy.

Microscopically, the two types of papillomas consisted of similar components but were easily differentiated. The pedunculated papillomas had an outer layer of thickened, relatively regular, but folded, hyperplastic epidermis capped by varying amounts of keratinized cells and keratinaceous debris. This layer, 10 to 20 epithelial cells thick, rested on an inner layer of connective tissue stroma. The dermis within the stalk was often more fibrous and denser than normal, and it generally contained minimal to occasionally severe inflammatory cell infiltrates. The broad-based papilloma (Fig. 3) had similar components, but the lesion lacked a stalk and was less protuberant, having a height less than the diameter of the base of the neoplasm. In both types of papillomas, the cells of the stratum granulosum of the epithelium were often arranged in regular masses, with ridges that were often severely elongated and that extended deeply into the dermis. The base of the rete ridges was well organized, and the cells were clearly demarcated from the adjacent dermis without interruption of the basement membrane (Fig. 4). The neoplasms contained few mitotic figures, and the cells were of similar size, shape, and staining qualities. Sectioning artifacts must be considered when examining the base of these lesions, the site where malignant changes most frequently occur. Sometimes nests of cells appeared to be separated from the rete pegs, suggesting metastases, but close examination of the cell size, shape, and staining properties indicated that the cell clusters did not represent early metastases but occurred rather as a function of cut.

The second type of benign neoplasm of epithelial cell origin commonly observed in SENCAR mice was keratoacanthoma. These neoplasms, referred to as inverted papillomas, developed in the dermis and arose from the

epithelial cells associated with hair follicles. The keratoacanthomas observed in the Matrix studies presented a wide variety of gross appearances. Most frequently, these neoplasms were crater-like and were filled with keratin and surrounded by an irregular lip of abruptly reflexed and compressed epidermis (Fig. 5). Keratoacanthomas were generally irregularly round, and when situated superficially on the skin, the lesion, which had a bud-like appearance, pushed completely above the surface and rested on an appendage of stroma in a manner similar to pedunculated papillomas. As reported by Bogovsky, the keratoacanthoma is not always easily distinguishable from the papilloma. It is speculated that in these cases, the glabrous epidermis and the epithelium associated with the hair follicle simultaneously respond to the carcinogenic action of the same agent (19).

Ghadially (23,24) identified three types of keratoacanthomas in the mouse. Type 1 neoplasms arose from the upper part of the hair follicle, and types 2 and 3 developed from the lower part. Although we have not routinely attempted to characterize keratoacanthomas as to type, it is our experience that approximately half of these neoplasms in SENCAR mice are consistent with Ghadially's type 1 tumor, in that they were superficially located and often pedunculated. The remainder of the keratoacanthomas were embedded in the skin as shown in Figure 5. These neoplasms, consistent with the type 3 tumors described by Ghadially, were clinically more difficult to diagnose and were often misinterpreted as ulcers or, in some cases, as small squamous cell carcinomas.

Descriptions such as "cup- or berry-shaped," commonly used to describe keratoacanthomas, were best appreciated when the lesions were examined microscopically (Fig. 6). The sides of the tumor were convex and were composed of sheets of compressed epithelial cells. Generally, the central core of the lesion was filled with laminated keratin interrupted only by an occasional frond of epithelial cells. Unlike papillomas, the amount

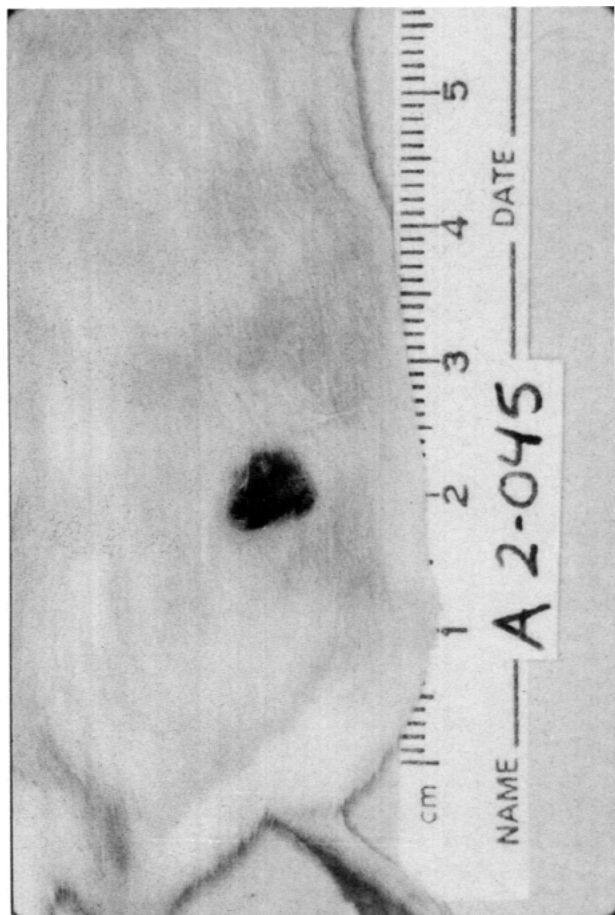


FIGURE 5. Keratoacanthoma. Irregularly round slightly raised neoplasm having a central crater surrounded by an elevated rim of epidermal tissue.

of keratin and keratinaceous debris was usually the predominant component in these lesions. Both trichohyaline and keratohyaline granules were seen in the epithelium. The base of the lesion was situated either in the dermis or subcutis, often resulting in marked displacement and compression of the stroma. This lesion differs from the squamous cell papilloma in that the dermis immediately beneath the papilloma was usually thicker and denser. In both papillomas and the keratoacanthomas, malignant transformation was observed to occur most often at the base of the neoplasms. Early transformation was characterized by penetration of the compressed dermis and invasion of the muscle layer by nests of irregular cells, distinguished by showing variation in size, shape, and staining qualities. These changes, since they frequently occurred at the base of the tumor and were hidden from gross observation, were seldom diagnosed as malignant lesions except in those cases where significant new tumor growth had pushed to the surface of the skin, causing an elevation of the peripheral portions of the tumors.

A review of the clinical and pathological data generated by several of the EPA's Matrix studies indicated that there was a direct correlation between the severity

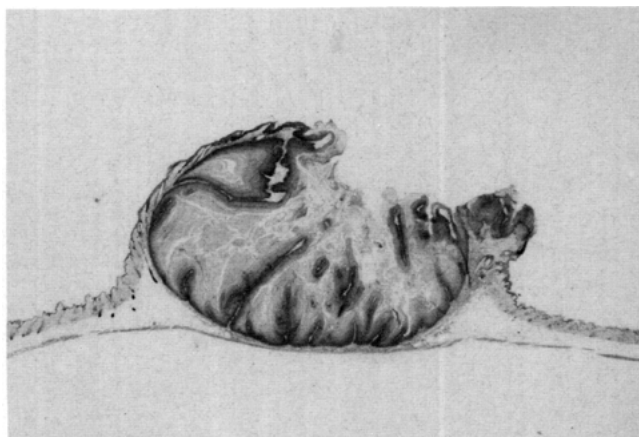


FIGURE 6. Keratoacanthoma. Classic cup-shaped keratoacanthoma. There is sharp demarcation between the margins of the tumor and the adjacent subcutaneous tissue (H & E, $\times 26$).

of ulceration during the initial stages of promotion and the incidence of keratoacanthomas. Although the dose of TPA administered in the various Matrix studies did not change, some inconsistency was observed in the response of the skin to promotion. In shipments of mice in which there was early and persistent ulceration in response to promotion, the incidence of keratoacanthomas increased significantly and approximated the number of squamous cell papillomas that developed. In these cases, the malignant transformation of keratoacanthomas was also increased.

The neoplasm with the most variable gross appearance was the squamous cell carcinoma. The classic features of a carcinoma are shown in Figure 7. These neoplasms arose from pre-existing papillomas, keratoacanthomas, or epidermal inclusion cysts developed spontaneously within the epidermis, initially as carcinoma *in situ*, or developed in association with ulcers. If the carcinomas are examined microscopically in the early stages of tumor development, the origin of the lesion can be determined. The most consistent features observed in the carcinomas in our studies were severe ulceration, crater formation, and rapid growth. The last feature was typically demonstrated by a rapid and striking elevation of the margins of the tumor, with the borders becoming indurated and poorly defined.

Based on microscopic features of the neoplasms, three types of squamous cell carcinomas have been previously identified: (1) keratinizing, (2) nonkeratinizing, and (3) anaplastic (19). The appearance of these neoplasms was greatly influenced by the origin of the malignant lesion. In the EPA Matrix studies, the majority of the carcinomas that developed were keratinizing types. However, it is our experience that the factors that affected the development of keratoacanthomas similarly influenced the type of carcinoma that developed. Those animals with initially severe ulceration persisting throughout the promotion phase developed carcinomas that were invariably less keratinized and more anaplastic.

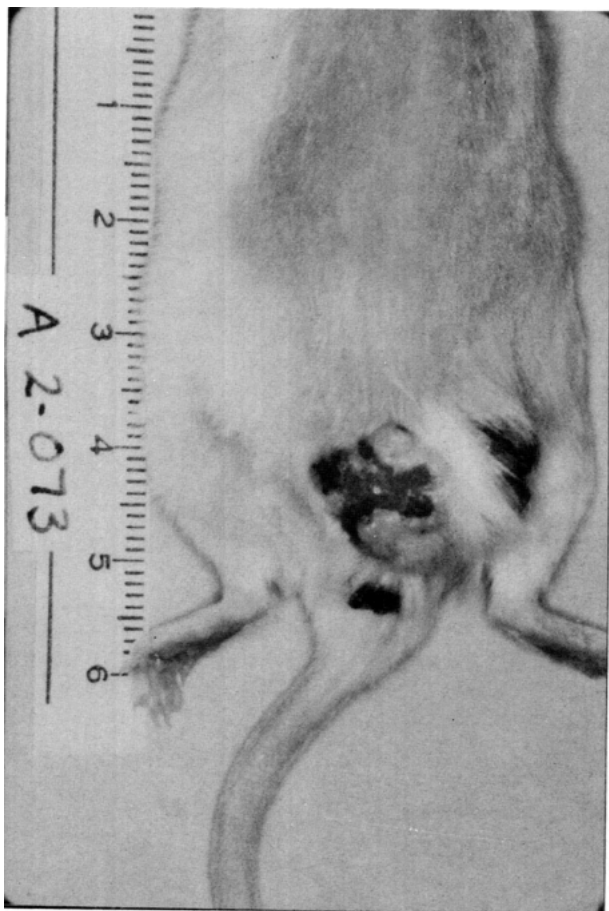


FIGURE 7. Squamous cell carcinoma. Carcinoma with crater formation, central ulceration with the margins formed by a rim of elevated malignant epidermal tissue.

In these cases, the carcinomas appeared to develop more frequently, either from ulcers or from within areas of epidermal hyperplasia, and without evidence that any benign tumors were present before the carcinoma developed.

Carcinomas developing from papillomas, keratoacanthomas, or epidermal hyperplasia were keratinized-type carcinomas, comprising differentiated and undifferentiated squamous cells arranged in cords or whorls with keratinized or partially keratinized centers (Fig. 8). The cords or fingerlike trabeculae extended into the underlying dermis, subcutis, and often into the subcutaneous muscle layers and vessels. The cells of these tumors were irregular in shape and size, and the nuclei were generally round or oval and of varying dimensions. The cells typically stained with varying intensity, with those cells at the margins of the neoplasms often being atypical, hypertrophied, and stained pink to brightly eosinophilic. As the carcinomas became less keratinized and more anaplastic, mitotic activity was increased, keratinization of single cells became more frequent, and intercellular bridges, commonly observed in well differentiated carcinomas, were more difficult to find. Figure 9 demonstrates an atypical squamous cell carcinoma.

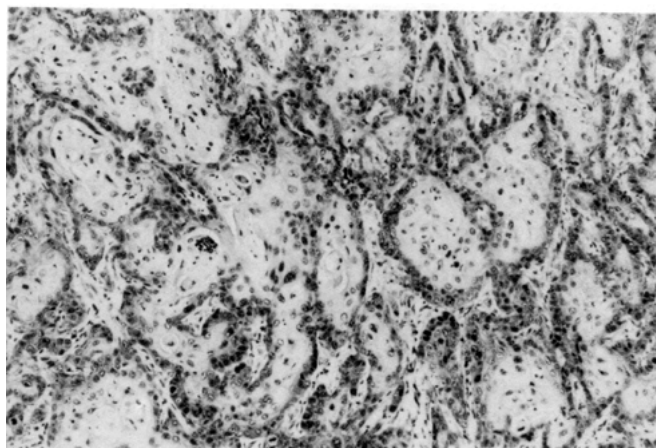


FIGURE 8. Squamous cell carcinoma. Differentiated and undifferentiated squamous cells are arranged in irregular cords and whorls with keratinized and partially keratinized centers (H & E, $\times 260$).

Poorly developed keratinized squamous elements and aggregates of atypical epithelial cells were observed, but the predominant cellular structures were the irregular whorls of poorly differentiated, elongated cells. These structures appeared to be forming rudimentary hair follicles with, occasionally, one to several cells in the central core undergoing keratinization.

Associated with the vast majority of carcinomas, regardless of type, was a moderate to severe chronic-active inflammatory process consisting of a mixed population of inflammatory cells and varying amounts of fibrosis. In some cases, there was a striking desmoplastic response, with the reactive connective tissue elements being the predominant structure in the neoplasm. Occasionally, the connective tissue elements of the neoplasms were highly irregular, poorly organized, and without orientation. Figure 10 shows such a neoplasm in which the sarcomatous-appearing stromal element

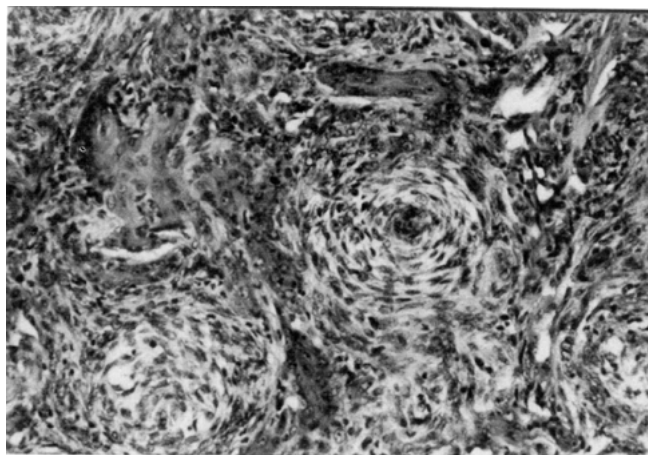


FIGURE 9. Squamous cell carcinoma. Anaplastic squamous cell carcinoma with irregular whorls of poorly differentiated elongated cells. Cells appear to be forming rudimentary hair follicles with keratinization of the core (H & E, $\times 260$).

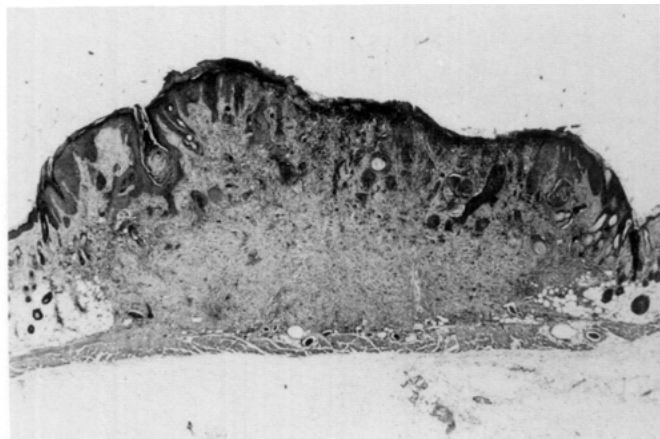


FIGURE 10. Squamous cell carcinoma. Carcinoma in which the sarcomatous appearing stromal element of the neoplasm occupies the majority of the lesion (H & E, $\times 52$).

occupies most of the lesion. In several cases, both the epithelial and the connective tissue elements appeared to have undergone malignant transformation, and carcinosarcoma was diagnosed. The pathogenesis of a neoplasm of this type is not understood. This neoplasm may represent two separate and distinct neoplasms that arise simultaneously or may represent a fibroepithelioma as described by Pinkus (25).

As was the case for several other types of tumors previously discussed, the carcinosarcomas appeared to develop only in those animals which had persistent ulceration in response to either the promotor or initiator. The presence of ulceration may have allowed for direct contact of the initiator or promotor with the underlying dermis. Clinically, most of these tumors were diagnosed as sores and there was no evidence of a tissue change other than ulceration (Fig. 11). The prominent fleshy rim of tumor growth normally associated with squamous cell carcinomas was missing.

Interestingly, these lesions were observed only in SENCAR mice that were sacrificed terminally (13 months of age) and not in any animals that died early in the study. This observation is in agreement with findings in whole-life mouse skin paint studies conducted in other laboratories (W. Sheldon, National Center for Toxicological Research, personal communication), studies in which, with time, fewer carcinomas were observed, and sarcomas were the predominant tumor type.

Only one basal cell tumor was observed in the Matrix SENCAR mice. This is in agreement with those of other investigators who report basal cell tumors are rare in mice (19,20). The one basal cell tumor noted in our studies was a malignant lesion, comprising irregularly round, basophilic cells arranged in dense packets. Within several of the cell clusters, primitive sebaceous differentiation was present.

The remainder of the neoplasms involving the skin were primarily confined to the dermis and subcutis and,

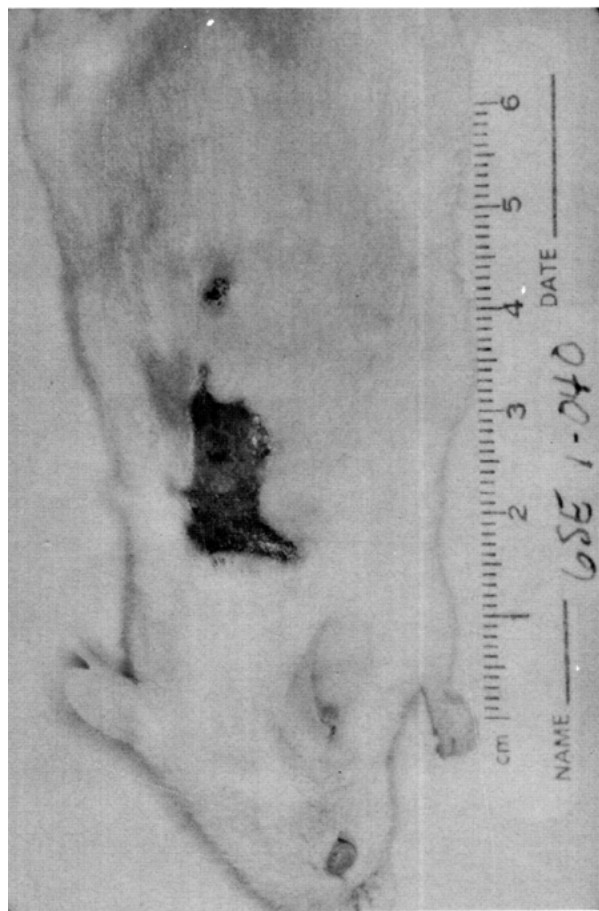


FIGURE 11. Squamous cell carcinoma. Ulceration, typical of a carcinoma is present, but the elevated rim of malignant tissue at the margins of the lesion is absent. Lesion was clinically diagnosed as a sore (ulcer).

with few exceptions, were diagnosed clinically as subcutaneous nodules. The vast majority of these lesions were mammary gland neoplasms including both benign and malignant neoplasms. Mammary gland neoplasms in mice have been classified by predominant cell type (26). The type-B mammary gland adenocarcinoma was the most frequent type observed. Mixed adenocarcinomas and adenoacanthomas were also common.

Among the other neoplasms observed in the subcutis were fibrosarcomas and rhabdomyosarcomas. With the exception of the carcinosarcomas described previously, the various sarcomas of the subcutis appeared to develop totally independently of the superficial aspects of the skin, and often only minimal epidermal changes accompanied the neoplasms. The incidence of the subcutaneous sarcomas was significantly increased in studies in which treatment was administered either by subcutaneous or interperitoneal injection versus the topical route of application. Only one plasma cell tumor was observed in the Matrix mice. Grossly, this neoplasm resulted in the irregular elevation of a substantial portion of the dorsal skin. Although the skin generally remained intact over the neoplasm, there was complete

Table 2. Classification of pulmonary lesions in female SENCAR mice.

Neoplasms	Nonneoplastic lesions
Primary neoplasms of the lung	Lymphoid infiltrates
Alveolar-bronchiolar adenoma	(peribronchiolar and perivascular)
Solid	Inflammation, interstitial
Papillary	Inflammation, granulomatous
Tubular	Histiocytosis
Alveolar	Myeloid hyperplasia
Mixed	Hyperplasia, alveolar lining cell
Alveolar-bronchiolar carcinoma	Hyperplasia, bronchiolar lining cell
Squamous cell carcinoma	
Secondary neoplasms of the lung	
Mammary adenocarcinoma	
Squamous cell carcinoma	
Histiocytic sarcoma	
Sarcoma, NOS	

loss of hair and severe erythema. Microscopically, loosely arranged sheets of plasma cells had infiltrated the dermis and subcutis. This infiltration was accompanied by a mild to moderate hyperplasia of the epidermis that consisted primarily of acanthosis. The epidermis was interrupted by multiple erosions and several small focal ulcerations.

Gross and Microscopic Lesions of the Lung

The pathological findings in several of the studies demonstrated an increased incidence of primary lung tumors in the SENCAR mouse in response to several known carcinogens as compared to that of vehicle controls. In most cases, this response was dose related. Based on these findings, Robinson and others (12) subsequently used the SENCAR mouse in combined bioassay studies in which a modified Shimkin lung adenoma assay and the skin papilloma assay were conducted simultaneously. During the past 30 months, the lungs from approximately 3500 SENCAR mice were examined microscopically. This examination included the lungs of mice used in combined bioassay studies and other skin initiation-promotion studies in which abnormal lung changes were recognized grossly. The various types of lesions that we observed in the SENCAR mouse lung are shown in Table 2.

Nonneoplastic Lesions of the Lung. Inflammatory lesions were the most frequently observed nonneoplastic changes observed in the lungs of SENCAR Matrix mice. These inflammatory responses varied in both morphologic features and severity, and in several studies, the changes were not always treatment and/or dose related. In this case, the lesions were nonspecific in origin. The most common lesion consisted of randomly distributed peribronchiolar and perivascular lymphocytic cellular infiltrates that generally involved one to several pulmonary airways and/or vessels. In some cases, the collar lymphoid infiltrates extended into the adjacent alveolar interstitium for short distances. Frequently, a small population of plasma cells accompanied these lesions. Similar changes have been observed in other

stocks and strains of mice and we regarded these changes as common, nonspecific, and incidental findings.

In several studies, the pulmonary response consisted of a more severe, chronic-active interstitial inflammation. Lymphocytes, plasma cells, and macrophages infiltrated the interstitium and early fibrosis of the alveolar septa often occurred. Varying numbers of foamy histiocytes occupied the alveolar spaces, and, occasionally, fewer numbers of neutrophils and lymphocytes were present. Associated with these changes was a minimal to mild hyperplasia of the alveolar lining cells. The morphologic features of these lesions were similar to those described as being caused by infectious agents, including Sendai infection (27). However, no definitive agent was identified by serologic examination of sentinel mice. These lesions, on gross examination, appeared as poorly defined, irregularly round, tan foci, and, when subpleural, they were slightly raised above the pleural surface of the lung. These subpleural changes were difficult to distinguish from primary lung tumors on gross examination and during the Shimkin counts.

Another type of inflammatory response observed was more granulomatous in nature and often included the formation of one to several granulomas that had varying degrees of organization. These lesions were occasionally quite large and were almost exclusively subpleural in distribution. The presence of these lesions was restricted to those mice which had severe skin ulcerations and/or ulcerated skin tumors. In these animals, granulomas or chronic inflammatory infiltrates were also frequently found in the kidney and/or liver. These lesions most likely represented a response to systemic infections that originated from the ulcerated skin. In the lung, the well-organized subpleural granulomas were routinely misinterpreted as primary lung tumors in that they were generally tan, well circumscribed, and elevated above the pleural surface of the lung, features consistent with pulmonary adenomas.

Histiocytosis, in the absence of other inflammatory response, was also a frequent observation in the lungs of both treated and nontreated SENCAR mice. This lesion, recognized routinely in other strains and stocks of mice, has been interpreted as an incidental, nonspecific change often associated with older mice (28). The lesions in the SENCAR mouse, in the absence of other inflammation or neoplasia, consisted of large histiocytes (macrophages) with abundant grey foamy cytoplasm and a single small dark nucleus. In mice with primary lung neoplasms, aggregates of histiocytes were found at the margins of tumors, especially in association with alveolar-bronchiolar carcinomas. In these cases, the cytoplasm of the histiocytes was brightly eosinophilic and the nucleus appeared pyknotic. The presence of cells of similar morphology have been reported in association with alveologenic tumors in many strains of mice (28). In the SENCAR mice, brightly eosinophilic histiocytes were also found associated with small focal areas of alveolar lining cell hyperplasia in which the alveolar spaces contained both histiocytes and a homogenous, proteinaceous material that most likely represented a

secretory product. When these lesions had a subpleural distribution, they were occasionally misinterpreted as primary lung tumors.

Myeloid hyperplasia was observed in the lungs of SENCAR mice that had severe, long-standing skin ulcers or ulcerated neoplasms. Mature and immature cells of the granulocytic series were found within alveolar capillaries and major pulmonary vessels. These lesions seldom had gross manifestations.

Hyperplasia of either alveolar lining cells and/or the bronchiolar epithelium was a common observation. These hyperplastic foci were most frequently observed in association with alveolar ducts, and to a lesser extent, with terminal bronchioles. They were seldom subpleural in distribution. Some investigators have previously classified the pulmonary hyperplasias by overall morphologic pattern and have included types such as solid, tubular, papillary, alveolar, etc. (29,30). The vast majority of the hyperplastic lesions observed in the SENCAR lung were of the alveolar and/or papillary-mixed types.

Neoplastic Lesions of the Lung. The morphologic and histogenic classification of primary pulmonary tumors in the mouse lung continues to be controversial. Most pathologists involved in mouse carcinogenesis studies have separated the alveolar-bronchiolar tumors into adenomas and carcinomas. However, it is generally accepted that pulmonary adenomas ultimately become malignant (31,32). In the SENCAR Matrix mice, both alveolar-bronchiolar adenomas and carcinomas were observed, but the majority of the primary lung tumors were adenomas. This finding was most likely influenced by the age of the mouse and the time on study, since all Matrix mice were sacrificed before 14 months of age, with some studies terminated before 12 months. Ward (29) and others (29-34) have classified the primary lung tumors according to morphologic arrangement. Alveolar, solid, papillary, tubular, and mixed types have been identified. In the SENCAR Matrix mice, approximately equal numbers of solid and papillary or papillary-mixed tumors were observed. The solid alveolar-bronchiolar adenomas were most frequently subpleural in distribution and were easily discernible on gross examination as pale, tan, well circumscribed, elevated nodules. Microscopically, these lesions consisted of tightly packed, nonciliated cuboidal cells that rested on scanty amounts of fine reticulin stroma. The borders of these neoplasms compressed the adjacent parenchyma and were often poorly defined and nonencapsulated. The majority of the papillary and/or papillary-mixed type adenomas were associated with small airways. In some cases, it was impossible to discern whether the tumors originated in the bronchiole or if the neoplasm had grown into the airway. In these lesions, the neoplastic cells were columnar, devoid of cilia, and uniform in size and shape. The borders of these lesions were also poorly defined. Neoplastic elements feathered into the adjacent parenchyma in a manner resembling hyperplastic epithelial growth.

The malignant primary lung tumors, alveolar-bron-

chiolar carcinomas, varied in size from small focal tumors consisting of highly anaplastic cells to large neoplasms that effaced entire lung lobes. In large tumors, it was not uncommon to see multiple morphologic patterns in one lesion. The majority of the carcinomas observed in the Matrix mice were mixed types and frequently airway-associated. Our observations indicated that the papillary- or papillary-mixed-type neoplasms were more likely to become malignant lesions than the subpleural solid tumors. In some of the smaller papillary or mixed tumors, small foci of anaplastic cells usually more basophilic than the adjacent tumor cells, were observed as islands within a well-differentiated adenoma. These islands very likely represented malignant transformation of the lung tumor, a finding previously described by Mori (35). Mild to occasionally severe desmoplastic response was associated with the larger carcinomas. Although vascular invasion by malignant cells was present, no metastases to other organs were observed.

The cell of origin for primary lung tumors in the mouse has also been much debated. Until recently, most investigators reported pulmonary tumors in the mice as arising from alveolar lining cells, more specifically, the type-II lining cell (28,31,32). However, the finding that some of the neoplasms arose in or adjacent to airways suggested that bronchiolar epithelial cells may be the origin for some pulmonary tumors. Kaufman et al. (33,34) first proposed the Clara cell as the cell of origin for tubular and/or papillary lesions that were most frequently airway associated. Most recently, Ward (29,30) used avidin-biotin immunocytochemical procedures to localize surfactant apoprotein (SAP) and Clara cell antigen (CCA) in both spontaneous and induced lung tumors in several strains and stocks of mice including the SENCAR mouse. These investigators found that the majority of the pulmonary tumors in the mouse were immunoreactive to SAP, a marker for alveolar type-II cells and that the Clara cell antigen could not be detected in any lung tumors, even in the papillary or tubular airway-associated tumors previously reported as being of Clara cell origin (33,34). It appears that the cell of origin for the solid, subpleural tumors and the papillary or papillary-mixed airway-associated neoplasms described in the SENCAR Matrix mice, remains controversial.

The only other primary lung neoplasm observed in the SENCAR mice was a squamous cell carcinoma. These tumors are extremely rare in mice (31) but have been induced by a number of polycyclic aromatic hydrocarbons (32). The one squamous cell carcinoma observed in the Matrix studies completely occupied one lobe and extended into the adjacent pleura. Microscopically, the neoplasm consisted of sheets of anaplastic cells, and numerous mitotic figures were present. Unlike previously reported squamous cell carcinomas (31), the neoplasm in the Matrix study contained only small amounts of poorly developed keratin with only limited formation of keratin pearls. Morphologically, this tumor resembled the foci of pulmonary squamous cell metas-

tases that were present in several mice with skin carcinomas. However, in the mouse with the primary neoplasm, no neoplastic lesions were present in either the skin or in the esophagus and forestomach.

Metastatic or secondary neoplasms involving the lung were observed in several of the Matrix mice. Metastases from mammary gland neoplasms and malignant skin lesions were most frequently observed. In these cases, the areas of metastases could not be differentiated, by gross examination, from primary pulmonary tumors.

Correlation of Gross and Microscopic Findings

During our discussion of the different types of lesions involving the skin and lung of the SENCAR Matrix mice, an attempt was made to define the gross and microscopic morphologic features that were most commonly associated with specific lesions. As part of the final pathology report that was generated for each Matrix study, a correlation table that compared the gross necropsy observations and the microscopic findings was prepared. Recently, we expanded the correlation of gross and microscopic data to include the clinical data recorded at the last observation period before terminal sacrifice. This observation occurred usually one week and not more than one month before sacrifice. Although a definitive statistical analysis of the correlation of the final clinical observation and microscopic data was not included in this report, a review of the clinical and microscopic data indicated that there were obvious shortcomings in the diagnostic accuracy of the gross observations.

It is our experience that even when the same personnel are used, their training maintained consistently, and the diagnostic criteria well established, many squamous cell skin neoplasms cannot be diagnosed accurately when only gross criteria are applied. Historically, attempts to correlate gross and microscopic diagnoses in skin initiation-promotion studies were neither performed nor reported, and when provided, the data were generally limited to confirmation of those lesions grossly determined to be carcinomas. It has been our experience that there was a high correlation between the lesions diagnosed grossly as squamous cell carcinomas and the microscopic findings. In these cases, the type of tumor and its malignant properties were generally easily recognizable. In one Matrix study, 18 of the 19 skin lesions diagnosed grossly as squamous cell carcinomas were microscopically confirmed as malignant neoplasms. Hennings (36) recently reported that more than 90% of the tumors diagnosed clinically as carcinomas were microscopically confirmed as squamous cell carcinomas. In most of these reports, the microscopic confirmation was limited to those lesions diagnosed grossly as carcinomas, which may explain the low conversion rates of papillomas to carcinomas that have been reported (37), since many of the lesions may have had subtle malignant changes that were not detected grossly and were never examined microscopically.

Correlation of clinical observations with microscopic findings also indicated that pedunculated squamous cell papillomas were also accurately diagnosed by gross examination, especially if the lesions were palpated carefully. The data from selected studies examined indicated that pedunculated squamous cell papillomas, as observed at the final clinical observation point, were diagnosed with 92% accuracy (44 of 48 papillomas).

The diagnostic accuracy of gross observations decreased markedly when other types of skin lesions were considered, particularly sessile papillomas, keratoacanthomas, and lesions diagnosed as sores. Almost half the sessile papillomas (12 of 26) and keratoacanthomas (four of ten) diagnosed grossly were microscopically confirmed to be squamous cell carcinomas. Six of ten lesions diagnosed grossly as sores were microscopically diagnosed as squamous cell carcinomas or carcinosarcomas. The reduced clinical diagnostic accuracy for lesions of this type can in part be explained by the fact that the early malignant transformation in these lesions most frequently occurred at the base of the lesion and was hidden from gross observation. It was not until the neoplastic cells extended upward and to the margins of the tumor was the malignant change appreciated grossly. It appears that the poor clinical diagnostic accuracy of lesions of this type is not limited to our laboratory. Ward reported that in three studies examined, there were three to four times more carcinomas diagnosed histologically than were found clinically, and he recommended that all skin tumors be examined microscopically when malignancy is a critical endpoint (30).

Figure 11 demonstrated a lesion diagnosed clinically as a sore that was actually a carcinosarcoma. If the rim of fleshy malignant tissue usually present at the margins of the ulcerated portion of a carcinoma was missing, the lesions were inaccurately diagnosed as a sore. We did observe that if the ulcerated lesion was dry and crusty, the lesion was more often an ulcer with epithelial hyperplasia rather than neoplasia. Occasionally, a skin lesion was observed to have the gross appearance of a small sessile papilloma (Fig. 12). Microscopically, however, although a superficial papilliferous protuberance was present, the base of the tumor consisted of a highly malignant squamous cell carcinoma that had invaded the subcutaneous muscle and body wall (Fig. 13). The anaplastic squamous cell carcinoma shown in Figure 9, clinically diagnosed as a papilloma, consisted of a superficial protuberance (Fig. 14) that was consistent with a papilloma. However, most of the lesion consisted of a highly anaplastic invasive carcinoma. It is unlikely that this lesion could have been diagnosed accurately without at least gross sectioning. Figure 15 shows the malignant conversion of a broad-based papilloma. In this case, the change was too subtle for gross detection.

Similarly, Figure 16 demonstrates the base of a neoplasm in which multiple islands of malignant cells developed separately from the base of the rete ridges, the area in which malignant transformation most frequently occurred. Figure 17 demonstrates even more vividly the frequent microscopic subtlety of malignant transfor-

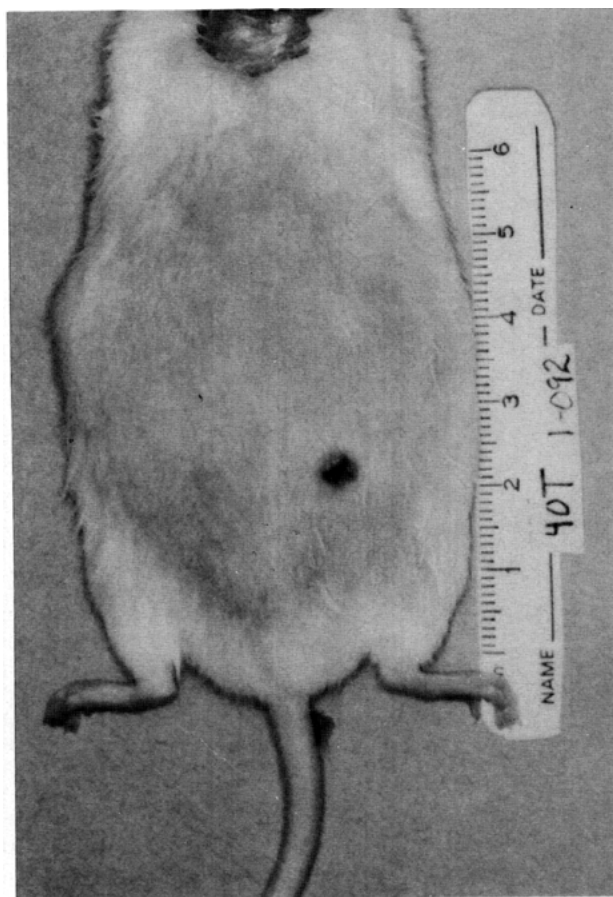


FIGURE 12. Squamous cell carcinoma. The lesion has the clinical presentation of a sessile papilloma. The malignant transformation at the base of the lesion was not observed grossly.

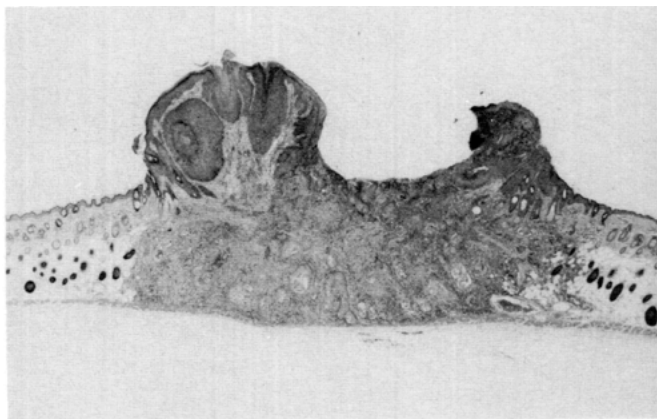


FIGURE 13. Squamous cell carcinoma. Microscopic appearance of the neoplasm in Fig. 12. Papillary protuberances border the lesion but there is invasion of the skin and body wall by the malignant neoplasm at the base of the lesion (H & E, $\times 52$).

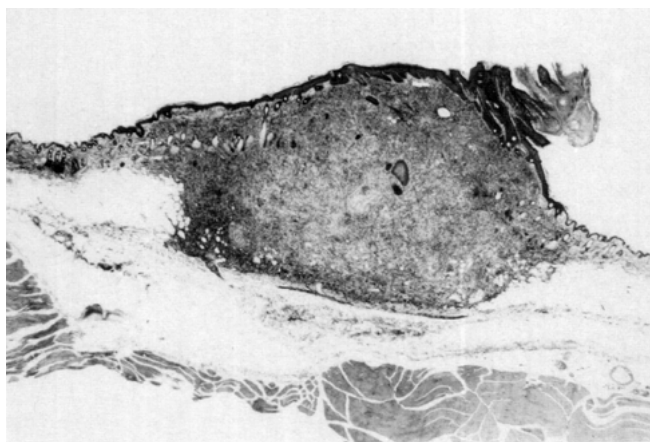


FIGURE 14. Squamous cell carcinoma. Lower magnification of anaplastic carcinoma in Fig. 9. The neoplasm had the superficial appearance of a typical, small papilloma (H & E, $\times 52$).

mation. Although junctional activity at the basement membrane was indicated, the definitive diagnosis of squamous cell carcinoma was made based on the two small aggregates of malignant cells. Multiple sections of this lesion were prepared, and in each, one or several small aggregates of malignant cells was observed.

Similar gross versus microscopic correlation difficulties were also encountered in studies of SENCAR Matrix mice lungs. In particular, while the modified Shimkin procedures were being performed as part of the combined bioassay studies, inflammatory lesions were misinterpreted as primary lung tumors. Subpleural granulomas and focal areas of chronic-active interstitial inflammation were commonly misinterpreted grossly as primary lung tumors, as were metastatic lesions from the skin, mammary gland, and other tissues. Accurate gross interpretation of the alveolar-bronchiolar tumors was further compromised by the distribution of the primary lung tumors. Approximately half the



FIGURE 15. Squamous cell carcinoma. Malignant transformation at the base (see arrow) of a sessile papilloma (H & E, $\times 52$).

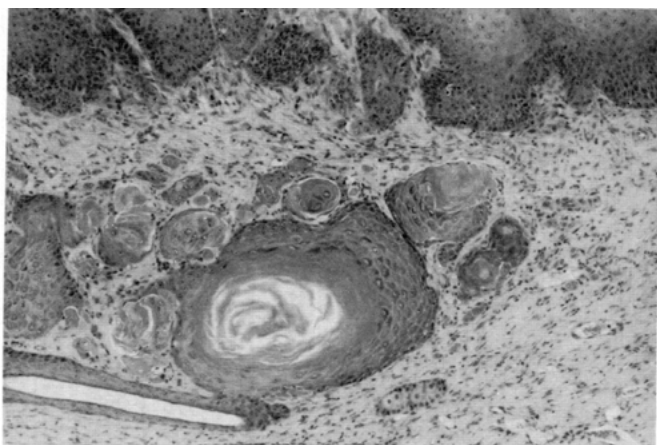


FIGURE 16. Squamous cell carcinoma. Several aggregates of malignant squamous cells at the base of a papilloma (H & E, $\times 130$).

lesions were loosely arranged papillary or papillary-mixed, airway-associated adenomas located deep in the lung parenchyma. This finding differs from those associated with the Strain A mouse routinely used in the lung adenoma assay in that the vast majority of the Strain A primary lung neoplasms were solid, well-defined, subpleural nodules and were easily recognized grossly (12–14). In one combined bioassay study in which both SENCAR and Strain A mice were used, only 30% of the lesions diagnosed grossly as tumors could be microscopically confirmed as primary lung neoplasms. Routinely, more than 75% of the lung tumors diagnosed grossly in the Strain A mice are microscopically confirmed. Not only does the subpleural location of the majority of the Strain A lesions aid in the accuracy of the Shimkin procedures, but also the inflammation present in the SENCAR mouse lung that frequently compromised gross diagnosis was not present in the Strain A mice. However, Robinson and others (12) have

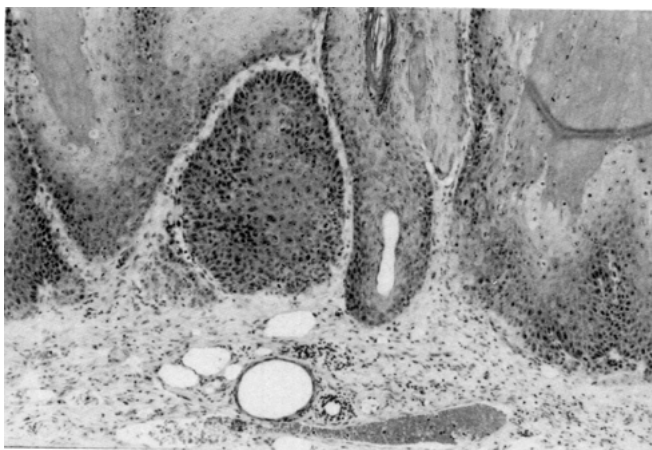


FIGURE 17. Squamous cell carcinoma. Subtle malignant transformation of a lesion at the base rete ridges. Note two small aggregates of malignant cells separate from the ridges (H & E, $\times 130$).

reported that after microscopic examination was performed on the lungs of treated SENCAR mice, the SENCAR mouse was only slightly less sensitive than the Strain A mouse in response to several known carcinogens and was significantly more responsive than other strains examined.

Conclusion

The gross and microscopic morphologic features of the various treatment-induced and spontaneously occurring lesions of the skin and lung of the SENCAR mouse have been reviewed. With few exceptions, there was generally poor correlation between the gross observations and the microscopic findings despite careful clinical observation and palpation. For the most part, gross versus microscopic discrepancies in the interpretation of skin lesions were attributed to the wide range of gross manifestations of the various lesions and to the fact that when there was apparent malignant transformation of benign skin neoplasms, it most frequently occurred at the base of the lesion and could not be detected initially by gross observation. In the lung, non-neoplastic treatment-associated, and spontaneous background lesions often compromised accurate gross interpretation of primary lung tumors. However, the results of combined bioassay studies indicated that the SENCAR lung was responsive to several known carcinogens and that the SENCAR skin-lung tumor combined bioassay merits further consideration.

This material has been funded wholly or in part by the United States Environmental Protection Agency under contract 68-03-3170 to Pathology Associates, Inc. It has been subject to the Agency's review and it has been approved for publication as an EPA document. Mention of trade names or commercial products does not constitute endorsement or recommendation for use.

REFERENCES

1. Berenblum, I. The cocarcinogenic action of croton resin. *Cancer Res.* 1: 44–50 (1941).
2. Rous, P., and Kidd, J. G. Conditional neoplasms and subthreshold neoplastic states: a study of the tar tumors of rabbits. *J. Exptl. Med.* 73: 369–390 (1941).
3. Boutwell, R. K. Some biological aspects of skin carcinogenesis. *Progr. Exptl. Tumor Res.* 4: 207–250 (1964).
4. Boutwell, R. K. The function and mechanism of promoters of carcinogenesis. *CRC Crit. Rev. Toxicol.* 2: 419–447 (1974).
5. Van Duuren, B. L. Tumor promoting agents in two-stage carcinogenesis. *Progr. Exptl. Tumor Res.* 11: 31–68 (1969).
6. Hecker, E. Structure-activity relationships in diterpene esters irritant and cocarcinogenic to mouse skin. In: *Carcinogenesis, Vol. 2, Mechanisms of Tumor Promotion and Cocarcinogenesis* (T. J. Slaga, A. Sivak, and R. K. Boutwell, Eds.), Raven Press, New York, 1978, pp. 11–42.
7. Slaga, T. J., and Fischer, S. M. Strain differences and solvent effects in mouse skin carcinogenesis experiments using carcinogens, tumor initiators and promoters. *Progr. Exptl. Tumor Res.* 26: 85–109 (1983).
8. DiGiovanni, J., Slaga, T. J., and Boutwell, R. K. Comparison of a tumor-initiating activity of 7,12-dimethylbenz(a)anthracene and benzo(a)pyrene in female SENCAR and CD-1 mice. *Carcinogenesis* 1: 381–389 (1980).
9. Hennings, H., Debor, D., Wenk, M. L., Slaga, T. J., Former, B., Colburn, N. H., Bowden, G. T., Elgjo, K., and Yuspa, S. H.

- Comparison of two-stage epidermal carcinogenesis initiated by 7,12-dimethylbenz(a)anthracene or *N*-methyl-*N*-nitro-*N*-nitrosoguanidine in newborn and adult SENCAR and BALB/c mice. *Cancer Res.* 41: 773-779 (1981).
10. Yuspa, S. H., Spangler, E. F., Donahoe, R., Geusz, S., Ferguson, E., Wenk, M., and Hennings, H. Sensitivity to two-stage carcinogenesis of SENCAR mouse skin grafted to nude mice. *Cancer Res.* 42: 437-439 (1982).
 11. Bull, R. J., and Pereira, M. A. Development of a short-term testing matrix for estimating relations carcinogenic risk. *J. Am. Col. Toxicol.* 1: 1-15 (1982).
 12. Robinson, M., Bull, R. J., Knutsen, G. L., Shields, R. P., and Stober, J. A combined carcinogen bioassay utilizing both the lung adenoma and skin papilloma protocols. *Environ. Health Perspect.* 68: 141-146 (1986).
 13. Shimkin, M. B., and Stoner, G. D. Lung tumors in mice: application to carcinogenesis bioassay. *Cancer Res.* 21: 1-58 (1975).
 14. Stoner, G. D., and Shimkin, M. B. Strain A mouse lung tumor bioassay. *J. Am. Col. Toxicol.* Vol. 1, 1: 145-169 (1982).
 15. Slaga, T. J. Overview of tumor promotion in animals. *Environ. Health Perspect.* 50: 3-14 (1983).
 16. VanDuuren, B. L. Cocarcinogens and tumor promoters and their environmental importance. *J. Am. Col. Toxicol.* 1: 17-28 (1981).
 17. Pereira, M. A. Mouse skin bioassay for chemical carcinogens. *J. Am. Col. Toxicol.* 1: 47-82 (1981).
 18. Shubik, P., Baserga, R., and Ritchie, A. C. The life and progression of induced skin tumors in mice. *Brit. J. Cancer* 7: 342-351 (1953).
 19. Bogovsky, P. Tumors of the Skin. In: *IARC Sci. Publ.* 23, IARC, Lyon, 1979, pp. 1-40.
 20. Holland, J. M., and Fry, R. J. Neoplasms of the integumentary system and harderian gland. In: *The Mouse in Biomedical Research*, Vol. IV (H. L. Foster, D. J. Small, and J. G. Fox, Eds.), Academic Press, Inc., New York, 1982, pp. 513-528.
 21. Long, R. E., Knutsen, G. L., and Robinson, M. Myeloid hyperplasia in the SENCAR mouse: differentiation from granulocytic leukemia. *Environ. Health Perspect.* 68: 117-124 (1986).
 22. Kovatch, R. M., Knutsen, G. L., and Robinson, M. Naturally occurring nonneoplastic pathology in the female SENCAR mouse. *Environ. Health Perspect.* 68: 105-115 (1986).
 23. Ghadially, F. N. Experimental production of kerato-acanthomas in hamster and mouse. *J. Pathol. Bacteriol.* 77: 277-282 (1959).
 24. Ghadially, F. N. The role of the hair follicle in the origin and evaluation of some cutaneous neoplasms of man and experimental animals. *Cancer (Philad.)* 14: 801-816 (1961).
 25. Pinkus, H. Epithelial and fibroepithelial tumors. *Arch. Dermatol.* 91: 24-37 (1965).
 26. Dunn, T. B. Morphology of mammary tumors in mice. In: *The Physiopathology of Cancer* (F. Homburger and W. Fishman, Eds.), Hoeber, New York, 1959, pp. 38-84.
 27. Hall, W. C., Lubet, R. A., Henry, C. J., and Collins, M. J. Sendai virus—disease process and research complications. In: *Complications of Viral and Mycoplasmal Infections in Rodents to Toxicology Research and Testing* (T. Hamm, Ed.), Hemisphere Publishing Co., Washington, DC, 1986, pp. 25-52.
 28. Ward, J. M., Goodman, D. G., Squire, R. A., Chu, K. C., and Linhart, M. S. Neoplastic and nonneoplastic lesions in aging B6C3F1 mice. *J. Natl. Cancer Inst.* 63: 849-854 (1979).
 29. Ward, J. M., Singh, G., Katyal, S. L., Anderson, L. M., and Kovatch, R. M. Immunocytochemical localization of the surfactant apoprotein and Clara cell antigen in chemically induced and naturally occurring pulmonary neoplasms of mice. *Am. J. Pathol.* 118: 493-499 (1985).
 30. Ward, J. M., Rehm, S., Devor, D., Hennings, H., and Wenk, M. L. Differential carcinogenic effects to skin and internal tissues by intraperitoneal 7,12-dimethylbenz(a)anthracene or urethane and topical initiation with 12-O-tetradecanoylphorbol-13-acetate promotion in female SENCAR and BALB/c mice. *Environ. Health Perspect.* 68: 61-68 (1986).
 31. Reznik, G. Spontaneous primary and secondary lung tumors in the mouse. In: *Comparative Respiratory Tract Carcinogenesis* (H. M. Reznik-Schuller, Ed.), CRC Press Inc., Boca Raton, FL, 1983, pp. 117-130.
 32. Stewart, H. L., Dunn, T. B., Snell, K. C., and Deringer, M. H. Tumors of the respiratory tract. In: *IARC Sci. Publ.* II, IARC, Lyon, 1979, pp. 251-287.
 33. Kauffman, S. L., Alexander, L., and Sass, L. Histological and ultrastructural features of the Clara cell adenoma of the mouse lung. *Lab. Invest.* 40: 708-716 (1979).
 34. Kauffman, S. L. Histogenesis of the papillary Clara cell adenoma. *Am. J. Pathol.* 103: 174-180 (1981).
 35. Mori, K., and Hirafuku, I. Histogenesis of lung carcinoma in mice induced by 4-nitroquinoline 1-oxide: carcinoma arising from areas of adenoma. *Gann* 55: 205-209 (1964).
 36. Hennings, H. Modified initiation/promotion schedule to enhance carcinoma development—a strain comparison. Workshop on the SENCAR Mouse in Toxicological Testing, Environmental Protection Agency, Cincinnati, Ohio (1985).
 37. Shubik, P. Progression and promotion. *J. Natl. Cancer Inst.* 73: 1005-1011 (1984).